

Do crossover functions depend on the shape of the interaction profile?

E. LUIJTEN^{1,2} and K. BINDER²

¹ *Max-Planck-Institut für Polymerforschung
Postfach 3148, D-55021 Mainz, Germany*

² *Institut für Physik, WA 331, Johannes Gutenberg-Universität
D-55099 Mainz, Germany*

(received 7 April 1999; accepted 1 June 1999)

PACS. 05.70.Jk – Critical point phenomena.

PACS. 64.60.Fr – Equilibrium properties near critical points, critical exponents.

Abstract. – We examine the crossover from classical to non-classical critical behaviour in two-dimensional systems with a one-component order parameter. Since the degree of universality of the corresponding crossover functions is still subject to debate, we try to induce non-universal effects by adding interactions with a second length scale. Although the crossover functions clearly depend on the range of the interactions, they turn out to be remarkably robust against further variation of the interaction profile. In particular, we find that the earlier observed non-monotonic crossover of the effective susceptibility exponent occurs for several qualitatively different shapes of this profile.

Introduction. – In recent years, there has been a revived interest in the nature of the crossover from classical to non-classical (asymptotic) critical behaviour upon approach of the critical point. This crossover between two universality classes can be observed in a great variety of many-body systems, including pure fluids, polymer mixtures and micellar solutions, and is driven by the ratio between the reduced temperature $t \equiv (T - T_c)/T_c$ (where T_c is the critical temperature) and a system-dependent parameter G , the Ginzburg number. The dependence of observables on this ratio is described by so-called *crossover functions*. Compared to our knowledge of critical exponents, for which very accurate, consistent estimates are available from renormalization group (RG) calculations, series expansions, experiments and numerical calculations, the situation for non-asymptotic critical phenomena is not so clear-cut. Most theoretical predictions for crossover functions are obtained by means of RG-based methods. Examples include the work of Nicoll and Bhattacharjee [1], who used an RG-matching method to calculate crossover functions for the one-phase region ($T > T_c$) to second order in $\varepsilon = 4 - d$ (d denotes the spatial dimensionality), and of Bagnuls and Bervillier [2], who applied massive field theory in $d = 3$. The latter work was then extended to the two-phase region as well [3], although only for temperatures relatively close to T_c . Very recently, the approach of ref. [3] was used to calculate the full crossover function for the susceptibility exponent below T_c [4]. A more phenomenological approach has been taken by Belyakov and Kiselev [5],

who presented a generalization of first-order ε -expansions. Although the different methods vary in mathematical rigour, they all suggest that the crossover functions are *universal* functions of the ratio t/G , under the additional restriction $t \rightarrow 0$, $G \rightarrow 0$. This limit, which is referred to as *critical* crossover, implies that one must consider the limit in which the coefficient u of the quartic term in the Landau-Ginzburg-Wilson (LGW) Hamiltonian goes to zero (as can be realized, *e.g.*, in systems with a diverging interaction range [6]). Experimental systems evidently do not obey these restrictions: Here G is a fixed parameter and the crossover functions are obtained by varying t , where it is generally assumed that within the critical region, *i.e.* for t sufficiently small, one still observes a universal crossover. Recent work [7-9] has shown that this assumption is only partially correct. In this paper, we therefore examine the role of some of the parameters that might be held responsible for deviations from the field-theoretic crossover curves and show what degree of universality one may still expect.

Anisimov *et al.* [10] have suggested that, apart from the correlation length ξ , an additional (mesoscopic) length scale may determine the nature of the crossover behaviour for complex fluids. Based upon earlier work [11], a corresponding parametric crossover function was proposed and in refs. [7, 12] it was shown that this function of *two* variables can indeed describe the crossover of the susceptibility exponent for several experimental systems displaying qualitatively different behaviour. On the other hand, there are quite a number of experimental results that can be described in terms of the above-mentioned *single*-parameter functions, although it should be noted that only few experiments have yielded accurate results for the effective exponents, which are defined as the logarithmic derivatives of the crossover functions [13]. Furthermore, most experiments only partially cover the crossover region, which occupies several decades in the reduced temperature. Thanks to recent algorithmic developments, numerical methods can circumvent both of these limitations in an efficient way, which has already led to several notable results [8, 14, 15]. In particular, it was demonstrated in ref. [8] that the crossover function for the effective susceptibility exponent γ_{eff}^+ (pertaining to $T > T_c$) for three-dimensional systems with a *finite* interaction range R is steeper than the functions presented in refs. [2, 5]. The reason for this discrepancy lies in u not being small for small R . Whereas the *scale* of the crossover is determined by the Ginzburg number, the *shape* of the crossover functions is determined by u [9]. This makes it difficult to obtain an explicit expression for the crossover. One possibility is to invoke the description of ref. [7]. A (still somewhat phenomenological) fit to this description is indeed possible [9], but a further demonstration that the crossover functions depend on more than one parameter is clearly desirable. The numerical results presented in refs. [8, 14, 15] have been obtained for a block-shaped interaction profile (the so-called equivalent-neighbour model), where the interaction strength is kept constant within a radius R_m and zero beyond that. As long as the interaction has a finite range, different interaction profiles will lead to the same universal properties [6], but not necessarily to the same crossover functions. Thus, there is a twofold objective in studying the effect of a modified interaction profile. In the first place, we want to study the effect of introducing an additional length scale in the block-shaped interaction profile, in order to study its influence on the crossover functions. Secondly, this modification of the interaction profile allows us to examine, on a more general level, the dependence of crossover functions on the shape of the interaction profile and thus to shed some light on the universal nature of these functions.

Simulational aspects and determination of critical properties. – In order to maximize the numerical sensitivity to variations in the crossover function, we have restricted ourselves to the two-dimensional (2D) case only. An additional attractive aspect of this system is that the effective susceptibility exponent γ_{eff}^- exhibits a remarkable non-monotonicity [14]. It is well possible that such a peculiar property is particularly sensitive to variations in the interaction

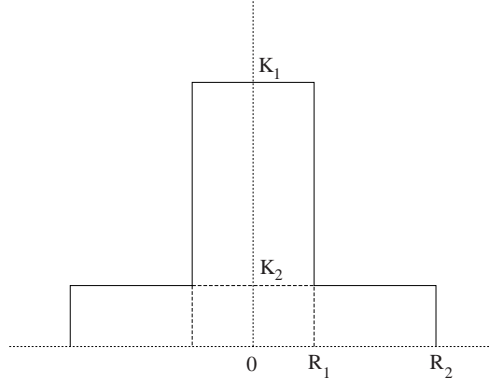


Fig. 1. – The interaction profile studied in this work. Each spin interacts with a ferromagnetic coupling K_1 with all its neighbours within a distance R_1 and with a coupling K_2 with those at a distance between R_1 and R_2 .

profile. Thus, we have carried out Monte Carlo simulations for a 2D Ising model, defined on a square lattice of size $L \times L$ with periodic boundary conditions. Each spin interacts with a strength K_1 with all its neighbours within a distance $r \leq R_1$ (domain D_1) and with a strength K_2 with all its neighbours within a distance $R_1 < r \leq R_2$ (domain D_2). This means that the block-shaped interaction profile of ref. [6] has been generalized to the double-blocked case depicted in fig. 1. The strength ratio K_1/K_2 is denoted by the parameter α , which throughout this work is supposed to be greater than unity. In order to suppress lattice effects, all range dependences are expressed in terms of the effective interaction range R , defined by

$$R^2 \equiv \frac{\sum_{i \neq j} |\mathbf{r}_i - \mathbf{r}_j|^2 K_{ij}}{\sum_{i \neq j} K_{ij}}, \quad (1)$$

which for our interaction profile reduces to $R^2 = (\alpha \sum_{i \in D_1} r_i^2 + \sum_{i \in D_2} r_i^2) / z_{\text{eff}}$, where $z_{\text{eff}} \equiv \alpha z_1 + z_2$, with z_i the number of neighbours in domain D_i . The strength ratio was chosen as $\alpha = 16$, in order to create a strong asymmetry between the two domains. The value of R_2

TABLE I. – *Some properties of the interaction profiles studied in this work. The systems are listed in order of increasing R , except for the last one, which is the only profile for which $R_1 < R_{\text{min}}$ ($R_1^2 = 27$ is the borderline case corresponding to the minimum in R).*

R_1^2	R_2^2	R^2	z_1	z_2	$\alpha z_1 / z_2$	K_c	Q	y_h
2	10	2.54	8	28	4.57	0.00872817 (2)	0.8559 (3)	1.8744 (9)
6	32	6.60	20	80	4.00	0.002918960 (7)	0.8566 (8)	1.8739 (14)
25	32	13.38	80	20	64.00	0.000836683 (2)	0.8551 (8)	1.8738 (13)
27	140	28.06	88	348	4.05	0.000598920 (2)	0.856 (2)	1.873 (2)
49	140	31.41	148	288	8.22	0.0003934150 (11)	0.858 (3)	1.872 (6)
70	140	39.32	220	216	16.30	0.0002775163 (9)	0.856 (5)	1.873 (3)
93	140	48.80	292	144	32.44	0.0002140278 (7)	0.856 (5)	1.878 (4)
114	140	57.91	356	80	71.20	0.0001777575 (4)	0.850 (4)	1.867 (5)
4	140	49.99	12	424	0.45	0.001683755 (5)	0.859 (4)	1.873 (5)

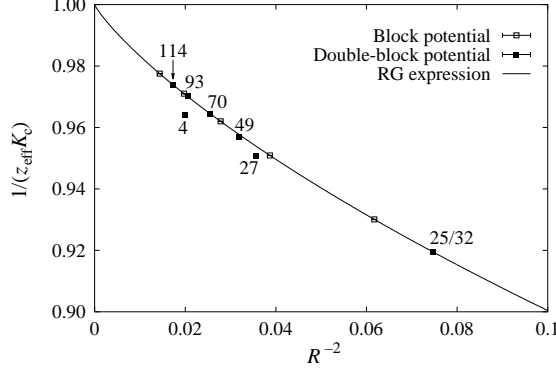


Fig. 2. – The critical temperatures of the various models as a function of the interaction range. The open squares and the curve refer to the block-shaped profile of ref. [6] and the black squares to the profiles studied in the present paper. The numbers indicate the value of the parameter R_1^2 (with $R_2^2 = 140$ fixed); the indication 25/32 refers to the system with $R_1^2 = 25$ and $R_2^2 = 32$.

was kept fixed at $\sqrt{140}$. In the finite-size scaling analyses, the minimum system size has to be of the order of R_2^2 and a maximum linear system size $L = 1000$ thus implies that the results cover a factor 7 in L . The effective interaction range R was then varied by varying R_1 . Both for $R_1 \rightarrow 0$ and for $R_1 \rightarrow R_2$, R will take its maximum value (which in the continuum limit approaches $R_2/\sqrt{2}$) and it will reach a minimum at $R_1 = R_{\min}$. In the continuum limit, the corresponding effective range is $R^2 = R_{\min}^2 = R_2^2/(\sqrt{\alpha} + 1)$. Although the same values for R can be reached with $R_1 < R_{\min}$ and $R_1 > R_{\min}$, it should be noted that the two cases greatly differ. For example, for $R_2^2 = 140$ and $\alpha = 16$ (where $R_{\min}^2 = 28.06$ is reached for $z_1 = 88$, *i.e.* $26 \leq R_1^2 \leq 28$) one may obtain $R^2 \approx 50$ by choosing either $R_1^2 = 4$ or $R_1^2 = 93$, but in the former case D_1 contains 12 out of 436 interacting neighbours, compared to 292 out of 436 in the latter case. This means that the integrated coupling ratio $\alpha z_1/z_2$, which indicates the relative contribution of the two domains to the total integrated coupling, is 0.45 in the first case and 32 in the second case. So, in combination with the original block-shaped profile, we can realize three qualitatively different interaction profiles and study the dependence of the crossover curve on the profile. Table I lists some properties of the interaction profiles considered in this work. The three profiles with $R_2^2 < 140$ were added in order to reach very small effective interaction ranges as well. For each choice, we have carried out extensive simulations using a dedicated cluster algorithm for long-range interactions [16]. The critical properties of each individual system were determined via finite-size scaling analyses, along the lines described in ref. [6]. The critical coupling, for which an accurate value is required to attain the proper crossover curve, has been determined from the amplitude ratio $Q = \langle m^2 \rangle^2 / \langle m^4 \rangle$ and we have obtained the magnetic exponent y_h from the absolute magnetization density $\langle |m| \rangle$ (see table I). One notes that for all systems Q is in good agreement with the 2D Ising value $Q_1 \approx 0.856216$ [17] and y_h lies very close to $15/8$. This confirms the expectation that all systems belong to the 2D Ising universality class. In addition, we have determined the magnetic susceptibility for $t < 0$ from the fluctuation relation $\chi = L^d(\langle m^2 \rangle - \langle |m|^2 \rangle) / k_B T$ and the critical finite-size amplitudes of $\langle |m| \rangle$ and $\langle m^2 \rangle$.

Range dependence of critical properties and analysis of the crossover functions. – Figure 2 shows the critical temperatures as a function of the interaction range. All temperatures are expressed in units of the critical temperature of the mean-field model, $T_c = 1/(z_{\text{eff}} K_c)$.

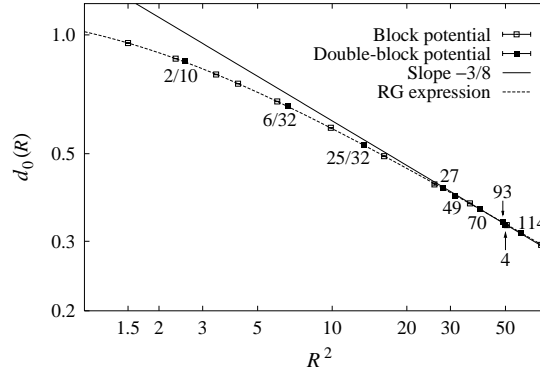


Fig. 3. – Critical finite-size amplitude of the absolute magnetization density. The dashed curve indicates the RG expression fitted to the open squares; clearly, it also describes the black squares (referring to the interaction profiles of the present work) very well. The numbers are explained in the caption of fig. 2.

Since fluctuations are less suppressed when the interaction range decreases, one observes that T_c is gradually depressed for smaller R . More importantly, the figure illustrates that a definitely non-universal quantity like T_c does not depend on the effective interaction range alone: Although for several systems the critical temperature lies on the curve describing $T_c(R)$ for the block-shaped interaction profile, the systems with $R_1 \lesssim R_{\min}$ ($R_1^2 = 4, 27$) exhibit a clear deviation from this curve. Apparently, the latter systems show (for a given R) the greatest deviation from the mean-field model, in the sense that the suppression of fluctuations is least efficient.

In contrast, no such deviations are observed for the critical finite-size amplitude of, *e.g.*, the absolute magnetization density. This quantity, defined as $d_0 \equiv \lim_{L \rightarrow \infty} L^{d-y_h} \langle |m| \rangle$, has an asymptotic range dependence proportional to $R^{(3d-4y_h)/(4-d)}$ [6]. It turns out that the systems investigated in this work do not only follow this asymptotic law, but also for smaller R agree very well with the range dependence found for the block-shaped profile, see fig. 3. This even holds for highly asymmetric profiles such as $R_1^2 = 4$, $R_2^2 = 140$.

The quantity of central interest, however, is the magnetic susceptibility χ below T_c . In fig. 4 the crossover function for the block-shaped profile is shown as a reference curve. The parameter along the horizontal axis is proportional to t/G ($G \propto R^{-2d/(4-d)}$) and the susceptibility is divided by a factor R^2 to obtain a data collapse for different ranges. One clearly observes how the solid curve interpolates smoothly, but with a *non-monotonic* derivative, between the Ising asymptote and the classical asymptote. Within the same figure, we have also plotted the finite-size data for four different double-block profiles. Several remarks are in order here. First, all data have been divided by a range-dependent factor describing the deviation of the connected susceptibility from its asymptotic range dependence. This is similar to the difference between the dashed curve and the solid line in fig. 3; as this curve turns out to depend solely on the value of R and not on the *shape* of the interaction profile, it is permissible to use the same expression for all systems. For large interaction ranges, the correction factor approaches unity. Secondly, at the right-hand side of the graph the data points start to deviate from the reference curve. This is caused by the fact that, sufficiently close to T_c , the diverging correlation length is truncated by the finite system size. For the systems with $R_1^2 = 4$ and $R_1^2 = 93$ (both with $R_2^2 = 140$) this happens in the figure at different temperatures, despite the fact that they have very similar values for the effective range R . The reason for this is that the data points pertain to different system sizes, *viz.* $L = 1000$ and $L = 300$, respectively. The inset shows that for

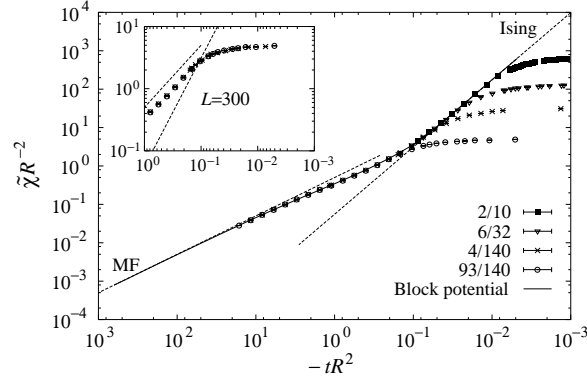


Fig. 4. – The crossover function for the connected susceptibility below T_c . $\tilde{\chi} = \chi/C(R)$, where $C(R)$ is a range-dependent correction factor that accounts for the fact that the critical amplitude for small R deviates from the asymptotic range dependence. This only introduces a shift along the vertical axis. The solid curve indicates the crossover function for the block-shaped interaction profile and the dashed lines mark the mean-field (MF) and the Ising asymptote. The numbers in the key refer to the values for R_1^2 and R_2^2 for each interaction profile. For clarity not all systems listed in table I have been included in the graph, but the omitted data points are fully compatible with those shown.

the *same* system size ($L = 300$) the data points for both systems virtually coincide, even in the finite-size regime! Finally, the left-most data points have been corrected for saturation effects, which are fully described by mean-field theory, cf. ref. [15]. This is merely an optical issue: Also the saturated curves (which display a strong decrease of the susceptibility) show no dependence on the shape of the interaction profile. The primary message, however, of fig. 4 is that for *all* interaction profiles the data in the thermodynamic limit perfectly coincide with the reference curve for the block-shaped potential. We view this as a strong indication that crossover functions possess a considerable degree of universality and conclude that a second length scale (R_1) of the form introduced in this work is insufficient to induce modifications of the crossover functions, contrary to some expectations.

Conclusions. – In summary, we have examined the critical properties of two-dimensional Ising-like models with an extended interaction range, for several different shapes of the interaction profile. In addition, we have calculated the crossover function for the susceptibility in the low-temperature regime, describing the crossover from classical to non-classical critical behaviour upon approach of the critical point. Although recent work has suggested that this function cannot be described in terms of a single parameter, namely the reduced temperature divided by the Ginzburg number, we find that it is independent of the precise shape of the interaction profile. Irrespective of the presence of an additional length scale or a high asymmetry in the interaction profile, all examined systems can be classified according to a single additional parameter describing the effective interaction range. In particular, the non-monotonic crossover of the effective susceptibility exponent, as found in ref. [14], is not a peculiarity of the block-shaped interaction profile, but can be observed for all systems studied in the present work, provided that the effective interaction range is sufficiently large. Furthermore, a corollary of the results presented here is that the coefficient u in the LGW Hamiltonian also appears to have only a weak dependence on the *shape* of the interaction profile. Of course, this still leaves the possibility that other parameters, that still need to be identified, have a more pronounced influence on u and thus on the crossover functions.

EL gratefully acknowledges illuminating discussions with M. A. ANISIMOV and J. V. SENGERS. We thank the HLRZ Jülich for computing time on a Cray-T3E.

REFERENCES

- [1] NICOLL J. F. and BHATTACHARJEE J. K., *Phys. Rev. B*, **23** (1981) 389.
- [2] BAGNULS C. and BERVILLIER C., *Phys. Rev. B*, **32** (1985) 7209.
- [3] BAGNULS C., BERVILLIER C., MEIRON D. I. and NICKEL B. G., *Phys. Rev. B*, **35** (1987) 3585.
- [4] PELISSETTO A., ROSSI P. and VICARI E., *Phys. Rev. E*, **58** (1998) 7146.
- [5] BELYAKOV M. Y. and KISELEV S. B., *Physica A*, **190** (1992) 75.
- [6] LUIJTEN E., BLÖTE H. W. J. and BINDER K., *Phys. Rev. E*, **54** (1996) 4626.
- [7] ANISIMOV M. A., POVODYREV A. A., KULIKOV V. D. and SENGERS J. V., *Phys. Rev. Lett.*, **75** (1995) 3146.
- [8] LUIJTEN E. and BINDER K., *Phys. Rev. E*, **58** (1998) R4060.
- [9] ANISIMOV M. A., LUIJTEN E., AGAYAN V. A., SENGERS J. V. and BINDER K., preprint cond-mat/9810252.
- [10] ANISIMOV M. A., KISELEV S. B., SENGERS J. V. and TANG S., *Physica A*, **188** (1992) 487.
- [11] CHEN Z. Y., ABBACI A., TANG S. and SENGERS J. V., *Phys. Rev. A*, **42** (1990) 4470.
- [12] MELNICHENKO Y. B., ANISIMOV M. A., POVODYREV A. A., WIGNALL G. D., SENGERS J. V. and VAN HOOK W. A., *Phys. Rev. Lett.*, **79** (1997) 5266.
- [13] KOUVEL J. S. and FISHER M. E., *Phys. Rev.*, **136** (1964) A1626.
- [14] LUIJTEN E., BLÖTE H. W. J. and BINDER K., *Phys. Rev. Lett.*, **79** (1997) 561.
- [15] LUIJTEN E., BLÖTE H. W. J. and BINDER K., *Phys. Rev. E*, **56** (1997) 6540.
- [16] LUIJTEN E. and BLÖTE H. W. J., *Int. J. Mod. Phys. C*, **6** (1995) 359.
- [17] KAMIENIARZ G. and BLÖTE H. W. J., *J. Phys. A*, **26** (1993) 201.